Bioactive Materials 18 (2022) 433–445

Contents lists available at ScienceDirect

Bioactive Materials

journal homepage: www.keaipublishing.com/en/journals/bioactive-materials

Sprayable nanomicelle hydrogels and inflammatory bowel disease patient cell chips for development of intestinal lesion-specific therapy

Hyo-Jin Yoon [a,1], Songhyun Lee [a,h,1], Tae Young Kim [a,b,1], Seung Eun Yu [a], Hye-Seon Kim [a], Young Shin Chung [c], Seyong Chung [a], Suji Park [a], Yong Cheol Shin [d], Eun Kyung Wang [e], Jihye Noh [f], Hyun Jung Kim [a,d], Cheol Ryong Ku [e], Hong Koh [f], Chang-Soo Kim [a,i], Joon-Sang Park [g,**], Young Min Shin [a,***], Hak-Joon Sung [a,*]

[a] Department of Medical Engineering, Yonsei University College of Medicine, Seoul, 03722, Republic of Korea
[b] School of Electrical and Electronic Engineering, Yonsei University, Seoul, 03722, Republic of Korea
[c] Department of Obstetrics and Gynecology, Institution of Women's Life Medical Science, Severance Hospital, Yonsei University College of Medicine, Seoul, 03722, Republic of Korea
[d] Department of Biomedical Engineering, The University of Texas at Austin, Austin, TX, 78712, USA
[e] Department of Internal Medicine, Endocrinology, Institute of Endocrine Research, Yonsei University College of Medicine, Seoul, 03722, Republic of Korea
[f] Department of Pediatrics, Gastroenterology, Severance Hospital, Yonsei University College of Medicine, Seoul, 03722, Republic of Korea
[g] Department of Computer Engineering, Hongik University, Seoul, 04066, Republic of Korea
[h] Institute of Tissue Regeneration Engineering (ITREN), Dankook University, Cheonan, 31116, Republic of Korea
[i] Numais Co., Ltd., Korea Seoul 04799, Republic of Korea

ARTICLE INFO

Keywords:
Nanomicelle
Injectable hydrogel
Peptide display
Theranostic
All-in-one treatment
Inflammatory bowel disease

ABSTRACT

All-in-one treatments represent a paradigm shift in future medicine. For example, inflammatory bowel disease (IBD) is mainly diagnosed by endoscopy, which could be applied for not only on-site monitoring but also the intestinal lesion-targeted spray of injectable hydrogels. Furthermore, molecular conjugation to the hydrogels would program both lesion-specific adhesion and drug-free therapy. This study validated this concept of all-in-one treatment by first utilizing a well-known injectable hydrogel that underwent efficient solution-to-gel transition and nanomicelle formation as a translatable component. These properties enabled spraying of the hydrogel onto the intestinal walls during endoscopy. Next, peptide conjugation to the hydrogel guided endoscopic monitoring of IBD progress upon adhesive gelation with subsequent moisturization of inflammatory lesions, specifically by nanomicelles. The peptide was designed to mimic the major component that mediates intestinal interaction with *Bacillus subtilis* flagellin during IBD initiation. Hence, the peptide-guided efficient adhesion of the hydrogel nanomicelles onto Toll-like receptor 5 (TLR5) as the main target of flagellin binding and Notch-1. The peptide binding potently suppressed inflammatory signaling without drug loading, where TLR5 and Notch-1 operated collaboratively through downstream actions of tumor necrosis factor-alpha. The results were produced using a human colorectal cell line, clinical IBD patient cells, gut-on-a-chip, a mouse IBD model, and pig experiments to validate the translational utility.

Abbreviations: IBD, inflammatory bowel disease; R&D, research and development; mPEG, methoxy poly (ethylene glycol); P(CL), poly(caprolactone); TNF-α, tumor necrosis factor-alpha; TLR5, Toll-like receptor 5; Pe, peptide; DSS, dextran sodium sulfate; TEM, transmission electron microscopy; SEM, scanning electron microscopy; DLS, dynamic light scattering; HPLC, high-performance liquid chromatography; TEER, transepithelial electrical resistance.

Peer review under responsibility of KeAi Communications Co., Ltd.

* Corresponding author.
** Corresponding author.
*** Corresponding author.
E-mail addresses: jsp@hongik.ac.kr (J.-S. Park), YMSHIN@yuhs.ac (Y.M. Shin), HJ72SUNG@yuhs.ac (H.-J. Sung).
[1] These authors contributed equally to this work.

https://doi.org/10.1016/j.bioactmat.2022.03.031
Received 10 November 2021; Received in revised form 7 March 2022; Accepted 20 March 2022

1. Introduction

A single medical item can exert multiple effects depending on its structural design and functional programming. Consequently, the repositioning of drugs and different devices has been investigated widely in the research and development (R&D) field of medical technologies. The R&D field is now moving to more advanced stages to equip one item with all necessary functions and effects ("All-in-one solution") [1], reflecting the state-of-the-art concept that we aimed to demonstrate technically in the present study. As a major point of innovation and impact, this study demonstrated a possibility to conduct a combination of monitoring, deployment, and treatment in a single step using experimental models of inflammatory bowel disease (IBD), representing a paradigm for future medicine. When an intestinal lesion is monitored by endoscopy, water injection is possible, together with the surgical removal of the polyp or tumor [2]. This process was reprogramed to inject hydrogels that could specifically adhere to and invade lesions. The hydrogel was designed to activate on-site therapeutic signaling via molecular conjugation without drug loading [3].

In detail, the hydrogel was used as a template to build a series of translatable functions as follows: (i) temperature-responsive solution to gel (sol-gel) transition for endoscopic injection [4]; (ii) nanomicelle formation of the gel status for nano-size-mediated lesion invasion to deliver and prolong therapeutic effects [5]; (iii) adhesive gelation to strengthen the intestinal barrier function after increased permeability by inflammatory disorders [6]; (iv) lesion-specific adhesion to intensify the therapeutic effects by minimizing unnecessary influences on non-lesion areas [7]; and (v) drug-free delivery of therapeutic effects into lesions specifically to remove side effects [8]. The (i) and (ii) functions were achieved by utilizing a well-characterized, widely studied hydrogel of a temperature-responsive di-block copolymer of methoxy poly (ethylene glycol) (mPEG) and caprolactone (CL). This hydrogel exhibited an efficient sol-gel transition at body temperature with nanomicelle formation and was previously used to inject therapeutics and cells [9]. The temperature responsiveness and physical properties of this hydrogel were also tunable by controlling the molar ratio between the PEG and PCL and the polymer concentrations [10].

Moreover, as the concept was shown previously [11], peptides were conjugated to this hydrogel as a touch-on signaling initiator, thereby programing the (iii-v) functions. *Bacillus subtilis* flagellin invades the intestinal epithelium during IBD pathogenesis and interrupts the barrier function [12]. Hence, the D1 domain of the flagellin was considered when designing the peptide candidates as a binding partner [13]. Toll-like receptor 5 (TLR5) is known to bind conserved domains including D1 in bacterial flagella; therefore, this information was applied to promote the peptide binding to TLR5, thereby silencing subsequent inflammatory signaling. TLR5 initiates a proinflammatory mechanism through tumor necrosis factor-alpha (TNF-α)-mediated downstream signaling, playing a key role in processing the proinflammatory action of Notch-1 [14], indicating synergistic anti-inflammatory signaling upon peptide binding. When gelation occurs upon injection, the hydrogel strengthens the barrier function of the intestinal epithelium, specifically in the infection lesions, and subsequently invades the epithelium to activate and prolong anti-inflammatory signaling through the anti-TLR5 and anti-Notch-1 mechanisms.

As limitations to report upfront, the lack of IBD porcine model resulted in no pre-clinical practice to monitor inflammatory gut regions by endoscopy and consequent insufficient validation of the theranostic mechanisms, including the barrier function in pigs. Despite continuous progress in IBD medicine, current treatment regimens, such as immunomodulators and biologic agents, still possess adverse side effects, as recognized in the clinic [15]. This study was focused on demonstrating the translational potential of the well-established hydrogel platform in combination with the practical concept of peptide functions. As other selling points of the present study, gut chips and IBD patient cells from the clinic were employed to validate the translation utility. The hydrogel was sprayed onto the intestine of pigs using the endoscopic function in addition to a mouse IBD model where the basic efficacy and efficiency of the approach were tested. The sellable value of this proof-of-concept study lies in that the drug-free therapy and operation of molecular docking-based anti-inflammatory signaling with potent propagation are suggested to be a promising alternative that could be utilized clinically in the future. The transitional potential of the suggested material platform with data validation of the concept should bring fresh impacts to the field regarding the repositioning and new combination of bioactive material factors towards the unexplored application.

2. Materials and methods

2.1. Computer simulation to determine the peptide binding target

Bacillus subtilis flagellin disrupts the barrier function of the intestine by interacting with the epithelium during activation of IBD. Consequently, the sequence of flagellin D1 domain was analyzed to identify peptide candidates to bind TLR5. In particular, the flagellin D1 domain serves as a primary and conserved binding site for TLR5, overexpressed in the epithelium upon inflammatory activation [13,16]. The interaction information was applied to select an ideal peptide so that TLR5-mediated inflammatory signaling could be suppressed. In a molecular docking study, five sequence candidates with varying lengths were analyzed by quantitatively comparing their binding affinities using the Schrödinger software suite [17]. The 3D structure of TLR5 protein (PDB ID: 3JOA) was retrieved from the Protein Data Bank (PDB) [18]. The TLR5 PDB file was processed with the Protein Preparation Wizard module, and the docking procedure was carried out using the Peptide Docking module [19] in the Schrödinger suite. As a result, various conformations of each peptide in the docking status with TLR5 were generated. The docking (Glide) score [17] and binding free energy were calculated using the molecular mechanics generalized born surface area (MM-GBSA).

2.2. Peptide (Pe)-hydrogel synthesis

A temperature-responsive di-block copolymer was synthesized via one-step ring-opening polymerization (ROP) of mPEG and CL, as reported previously [9]. First, mPEG (10 mmol) and CL (22 mmol) were prepared under vacuum to remove moisture in a three-neck round flask equipped with a stirring bar and submerged in an oil bath at 140 °C, followed by an ROP reaction using $Sn(Oct)_2$ as an initiator in diethyl ether with nitrogen purging for 1.5 h. The mPEG-PCL polymer was then dissolved in dichloromethane, precipitated in cold diethyl ether, and dried overnight under vacuum. The peptides (Lugen Sci. Co. Ltd, Bucheon, Korea) were then conjugated to mPEG-PCL via a 1,1′-carbonyldiimidazole (CDI)-mediated amination reaction as follows: (i) The hydroxyl group of mPEG-PCL (0.0130 mmol) was substituted with an imidazole leaving group via the SN2 reaction of CDI (0.0156 mmol) in dimethyl sulfoxide (DMSO; 10 mL) for 24 h, forming imidazole-carbamated MP. (ii) Ethylenediamine (ED: 0.0156 mmol) was conjugated to the imidazole-carbamated mPEG-PCL through imidazole displacement via an SN2 reaction in DMSO (10 mL) for an additional 24 h. The reactant was purified using a dialysis tube (cut-off: 100–500 Da) for three days. The obtained solution was lyophilized at −90 °C for 7 days and stored in a freezer (−20 °C) before use. (iii) Peptides were conjugated to aminated mPEG-PCL in a co-solvent of DMSO/distilled water (10 mL; 1:1 vol/vol) using 4-(4,6-dimethoxy-1,3,5-triazin-2-yl)-4-methyl-morpholinium chloride (DMT-MM) as a coupling agent, followed by purification and lyophilization in the same manner as for the aminated mPEG-PCL preparation.

2.3. Pe-hydrogel characterization

The structure and molar ratio of mPEG-PCL were determined using ^{1}H NMR spectroscopy (Avance III 400-MHz NMR spectrometer; Bruker Biospin, MA, USA) with $CDCl_3$ (0.03% vol/vol TMS). PCL peaks appeared at δ = 4.10 [m, –OCH_2], 2.41 [m, –CH_2], 1.74 [m, –CH_2], and 1.45 [m, –CH_2]; mPEG peaks were observed at δ = 4.13 [s, =CH_2] and 3.28 [s, =CH_2]; and peptide peaks were seen at δ = 1.70 [m, –CH_2] for arginine. The molar ratio of PCL to mPEG was determined by analyzing the ratio between the ^{1}H NMR absorption peak areas of PCL and mPEG. The molecular weight and polydispersity index (PDI) were determined by gel permeation chromatography (Agilent 1200 series; Agilent Technologies, CA, USA) against polystyrene standards using a PLgel 5 μm Mixed-D column (300 mm, Φ = 7.5 mm) in tetrahydrofuran at a flow rate of 1 mL min^{-1}.

2.4. Nanomicelle formation, sol-gel transition, and drug release of Pe-hydrogel

The nanomicelle formation of hydrogel was characterized by determining the mean diameter and PDI of micelles using dynamic light scattering (DLS, ELS-1000ZS, Otsuka Electronics Ltd., Osaka, Japan). The injectability of hydrogel was determined by examining the sol-gel transition at 37 °C using the tilting method with glass vials containing the solution of each test hydrogel, further characterized using a rheometer (Bohlin Advanced Rheometer, Malvern Instruments, Malvern, UK) with varying the gel concentration in the range of 10–60 °C.

In addition, scanning electron microscopy (SEM, MERLIN, Zeiss, Oberkochen, Baden-Württemberg, Germany) was used to examine the nanomicelle status of hydrogel (10 wt%) after it was immersed in liquid nitrogen and freeze-dried at −75 °C with a sputter coating (Emitech, K575, Tokyo, Japan). The nanomicelle morphology was also examined using transmission electron microscopy (TEM, H–6009IV, Hitachi, Japan) after diluting the samples with distilled water, placing them on a copper grid covered with nitrocellulose [20], conducting negative staining with phosphotungstic acid, and drying at room temperature (20–25 °C).

As a model drug, dexamethasone (Dex) was loaded into hydrogels at varying gel concentrations (6, 8, and 10 wt/vol%). A transwell was used to mimic the barrier function of the intestine, and the Dex release from the hydrogels was examined in the bottom well after penetration through the transwell membrane [21] for 48 h using high-performance liquid chromatography (HPLC; Agilent Technologies 1260 Infinity II system, Agilent Technologies Inc., CA, USA). In the bottom well, 5% Tween 80 in distilled water (DW) was added to facilitate the dissociation of Dex from hydrogel nanomicelles, and the amount of Dex was determined at each time point by analyzing the corresponding peak and retention time in comparison to the Dex standard curve.

2.5. Pe binding with targets by immunoprecipitation

Human colorectal adenocarcinoma (Caco-2) cells (American Type Culture Collection, Manassas, VA, USA) were cultured in Dulbecco's modified Eagle's medium (DMEM, Gibco, Grand Island, NY, USA) supplemented with 20% fetal bovine serum (FBS, Gibco) and 1% antibiotics in an incubator with 95% humidity and 5% CO_2 at 37 °C. TLR5 was overexpressed in the cells as a result of treating them with 4 mM butyrate (Sigma-Aldrich, St. Louis, MO, USA) for 24 h (Fig. S1).

Caco-2 cells (1×10^6 cells/mL) were subjected to immunoprecipitation (IP) using treatments with biotinylated 8 a.a peptide (20 μM, Bio-FD&C, Lugen Sci., Gyeonggi-do, Korea) at 37 °C for 24 h to determine the binding capacity with TLR5 and Notch-1. After lysing the cells with a buffer (Abcam, Cambridge, UK), the total protein was quantified using a BCA assay (Pierce Biotechnology, Rockford, IL, USA). Then, 1 mg of protein was incubated with Accunano-streptavidin magnetic beads (200 μL, Bioneer, Daejeon, Korea) to capture the biotinylated peptides by shaking at 4 °C for 24 h, followed by bead collection by discarding the supernatant and washing in phosphate-buffered saline (PBS) three times. Samples (45 μL) were subjected to sodium dodecyl sulfate-polyacrylamide gel electrophoresis (SDS-PAGE) for western blot analysis (see the section below) after resuspending in 50 μL of 2X SDS electrophoresis sample buffer and boiled for 5 min at 95 °C.

2.6. Co-localization of TLR5 and Pe-hydrogel by immunostaining

Preferable Pe-hydrogel co-localization with TLR5-overexpressed cells compared to normal cells was further validated by immunostaining. Fluorescein isothiocyanate (FITC) (Lugen Sci. Co. Ltd) was conjugated to the hydrogel to exert green fluorescence at Alexa 488 range and then used to treat cells with and without TLR5 overexpression. Cells were permeabilized with 0.3% Triton X-100 (Sigma-Aldrich) in PBS for 15 min and blocked with 5% bovine serum albumin (BSA, Hyclone Laboratories, Inc.) for 1 h. Samples were then incubated with primary mouse anti-TLR5 (1:100 dilutions; Abcam), washed with PBS containing 0.5% Tween 20, and incubated with secondary anti-rabbit conjugated to Alexa Fluor 594 (1:200 dilutions; Jackson ImmunoResearch Laboratories, PA, USA). Cell nuclei were counter-stained with NucBlueTM Live ReadyProbesTM Reagents (Invitrogen, Waltham, MA, USA), followed by confocal imaging (LSM780 or 700, Zeiss, Oberkochen, Land Baden-Württemberg, Germany) and image analysis using ImageJ (NIH).

2.7. Animals

All animal experiments were conducted following the Guide for the Care and Use of Laboratory Animals and were approved by the Institutional Animal Care and Use Committee (IACUC) of Yonsei University College of Medicine (authorization number; 2020–0202 (mice) and 2020–0264 (pigs)). Male C57BL/6 mice (5–6 weeks of age) were purchased from Orient Bio Inc. (Gyeonggi-do, South Korea), and they were then quarantined under specific pathogen-free (SPF) conditions with a 12 h light/dark cycle. Female Yorkshire race pigs (30–35 kg) were purchased from XP Bio (Gyeonggi-do, South Korea).

Colitis was induced in the mice by supplying them with drinking water containing 3% (w/v) dextran sodium sulfate (DSS, MW 36,000–50,000; MP Biomedicals, Seoul, South Korea) for 5 days. Mice were subjected to colitis resolution by overnight fasting and then intestinal injection of (Pe)-hydrogel (8% wt/vol) in PBS (vehicle control). Mice received normal drinking water for the next 13 days, and their body weight was checked daily until sacrificed by CO_2 asphyxiation. After harvesting the colorectal parts, the colon length was measured, and the colon tissues were cut longitudinally with PBS washing for histopathological examination. The distal sections of colon tissues were fixed in 10% formalin, whereas another portion was flash-frozen in liquid nitrogen and kept at −80 °C until further analyses.

The therapeutic effects of (Pe)-hydrogel on the intestinal barrier function were determined using hematoxylin and eosin (H&E) staining and immunostaining of tight junction markers, including zonula occludens-1 (ZO-1), occludin, and claudin-1 (Novus Biologicals, Littleton, CO, USA). Colon tissues were fixed in 10% formalin for 24 h, embedded in paraffin, sectioned (4 μm thickness), deparaffinized in xylene, and transferred to ethanol for rehydration. When necessary, antigen retrieval was conducted by heating samples twice for 6 min each in 10 mM citrate buffer (pH 6.0), and endogenous peroxidase activity and background staining were removed by treating samples with 3% hydrogen peroxide and 4% peptone casein blocking solution for 15 min. Tissue sections were incubated with primary antibodies (ZO-1, occludin, and claudin-1) at room temperature for 40 min in Tris-HCl-buffered saline containing 0.05% Tween 20. The samples were then incubated with horseradish peroxidase-conjugated secondary antibody (rabbit or mouse; Dako, Glostrup, Denmark), followed by fluorescence imaging (Leica DMi8, Leica Microsystems, Wetzlar, Germany).

Colonoscopies were conducted to inject hydrogel into the pig

intestine as a pre-clinical model to validate its translational utility (n = 2). Pigs were fasted for 24 h before the intervention, followed by an enema one hour before the procedure to clean the rectum and distal colon. A green fluorescent dye (Thermo Fisher Scientific) and Indian ink (NEXINK, Kyunggi-do, Korea) were encapsulated by Pe-hydrogel, and the injection function of colonoscopy was used to spray the sample to moisturize the pig intestine. Colon tissues were harvested 24 h after injection when the pigs were sacrificed, followed by histological examination of hydrogel invasion and intestinal barrier structure after fixing with 10% formalin, optical cutting temperature (OCT) embedding, sectioning (4 μm thickness), and optical imaging (Leica DMi8, Leica Microsystems).

2.8. IBD and normal patient cells

Patient tissue specimens were obtained from Yonsei Cancer Center (Seoul, Korea) with the approval of the Institutional Review Board (IRB) of Yonsei University College of Medicine (IRB No. 4-2018-0089) following the guidelines. Two Crohn's disease males provided the tissue samples to isolate cells in this study. The tissue samples were obtained from the inflamed ascending and sigmoid colons. Healthy (normal) and IBD lesion zones were resected within 1 h after harvesting fresh colonic tissues from patients at the time of surgery through biopsy. Cells were harvested from each zone after the tissues were washed with cold PBS three times, cut into pieces (<1 mm), and incubated with 20 mM EDTA solution at 4 °C with stirring for 1 h, followed by centrifugation at 150 ×*g* for 5 min at 4 °C. After adding TrypLE Express (3 mL, Gibco), they were incubated at 37 °C for 15 min. Enzymes were inactivated by adding DMEM supplemented with 10% FBS under gentle pipetting. After filtering the samples through a 40 μm cell strainer (Falcon, Durham, NC, USA), cells were collected by centrifugation at 400 ×*g* for 3 min and cultured until use.

2.9. Gut chip experiment using cell culture and cytokine secretion

A microfluidic device was produced using polydimethylsiloxane (PDMS; Sylgard 184, Dow Corning, Midland, MI, USA) by soft lithography, as was reported previously [22] to use the gut-on-a-chip method. Each (1.0 × 10 × 0.2 mm) of the upper and lower channels was generated by curing PDMS using a curing agent (15:1 w/w). The channels were separated using a PDMS membrane (20 μm thickness) containing an array of holes (10 μm diameter with 25 μm spacing). Culture media were supplied to each channel using a connector (a blunt-end needle, 18G, Kimble Chase, Vineland, NJ, USA) with silicone tubing (Tygon 3350, ID 1/32, "OD 3/32," Beaverton, OR, USA). Devices were sterilized using ethanol (70% vol/vol), dried at 60 °C, exposed to ultraviolet light for 30 min, and treated with O_2 plasma (PDC-32G-2, Harrik Plasma, NY, USA). For cell culture, the channels and membranes were coated with rat type I collagen (0.03 mg/mL; Gibco) and Matrigel (0.3 mg/mL; BD Biosciences, Bedford, MA, USA) in serum-free DMEM containing 4.5 g/L glucose for 1 h at 37 °C.

After washing the inside of chip channels with culture media, Caco-2 or patient cells (5 × 10^6 cells/mL) were seeded onto the membrane through the upper microchannel using a sterile syringe (1 mL Tuberculin slip tip; BD, Franklin Lakes, NJ, USA) and incubated at 37 °C in a humidified CO_2 incubator without flow for 1 h. Then, a monolayer of cells was formed by perfusing culture medium continuously through the upper microchannel at a constant flow rate (50 μL/h) with 0.02 dyne/cm^2 of shear stress) for 24 h using a syringe pump (Standard infuse/withdraw pump, Harvard Apparatus, Holliston, MA, USA). Next, both channels were perfused at a 40 μL/h constant flow for 5 days until villi generation. Secretion of the proinflammatory IL-6 and IL-8 through the media perfusion was determined using ELISA kits (Abcam) following the manufacturer's guidelines.

2.10. Epithelial barrier structure and function in gut chip

Cells on the gut chip were fixed with paraformaldehyde (4% wt/vol) for 15 min, permeabilized with Triton X-100 (3% vol/vol), blocked with BSA (2% wt/vol) for 1 h, and washed with Ca^{2+}-and Mg^{2+}-free PBS. The therapeutic effects of (Pe)-hydrogels on the epithelial barrier function were determined by immunostaining of the tight junction marker (ZO-1) with confocal imaging (LSM780, Zeiss). The cells were treated with the primary antibody ZO-1 (1:200, Novus Biologicals, Littleton, CO, USA) in an overnight incubation at 4 °C, followed by the secondary antibody, anti-rabbit IgG H&L conjugated with Alexa Fluor 488 (1:200, Abcam) in the dark for 3 h at room temperature. Then, confocal imaging was conducted (LSM780 or 700, Zeiss). Cell nuclei and F-actin were stained with NucBlueTM Live ReadyProbesTM Reagents (1:1000, Invitrogen) and Alexa Fluor 647 phalloidin (1:200, Thermo Fisher Scientific, Waltham, MA, USA), respectively, at room temperature for 30 min. After washing the samples with PBS, the villi structure was 3D reconstructed using z-stack images from confocal imaging with Zen software, and then the villi height was analyzed using ImageJ.

Villi formation was characterized additionally by phase-contrast imaging (EVOS XL Core inverted phase-contrast microscope, Life Technologies, Carlsbad, CA) of the 2D epithelial surface. As another indication of barrier function, transepithelial electrical resistance (TEER) was determined using a voltage-ohm meter (87V Industrial Multimeter, Fluke Corporation, Everett, WA, USA) in connection with Ag/AgCl electrode wires (0.008″ in diameter; A-M Systems, Inc., Sequim, WA, USA). After measuring the TEER in the absence of epithelium (Ω_b), cell culture was initiated with TEER measurement on day 0 (Ω_0), followed by the measurement (Ω_t) at each time point by calculating the normalized $\text{TEER} = (\Omega_t - \Omega_b)/(\Omega_0 - \Omega_b)$.

2.11. Notch-1 mechanism of Pe-hydrogel therapy in Caco-2 cells

Caco-2 cells (1 × 10^5 cells/mL) were cultured in DMEM supplemented with 20% FBS and 1% antibiotics in an incubator with 95% humidified air and 5% CO_2 at 37 °C. Inflammatory activation of the cells was induced by treating with TNF-α (10 ng/mL in DMEM) for 0, 6, 12, 24, and 36 h or with TNF-α (0, 5, 10, 50, and 100 ng/mL in DMEM) for 24 h, followed by determination of IL-6 and IL-8 expression in western blot analysis (see the section below). As a binding partner to both Notch-1 and TLR5, the therapeutic effects of Pe-hydrogels were examined in Caco-2 cells after treatment with TNF-α (10 ng/mL) for 24 h. After incubating with (Pe)-hydrogels (20 μM) for 24 h, the expression of the tight junction and Notch-1 signaling markers was examined using western blot analysis (see the section below). A mechanistic role of Notch-1 in the binding effect of Pe-hydrogel was confirmed by silencing Notch-1 expression via transfection of siRNA (25 nM) into Caco-2 cells using lipofectamine RNAiMAX (Invitrogen) before (Pe)-hydrogel treatment. The siRNA sequences were as follows: (forward) 5′ –GUG UGA AUC CAA CCC UUG U-3′ and (reverse) 5′ –ACA AGG GUU GGA UUC ACA C-3′ (Bioneer, Seoul, South Korea).

2.12. Western blotting

Cells were scraped in lysis buffer [150 mM NaCl, 0.5% Triton-X 100, 50 mM Tris-HCl (pH 7.4), 20 mM ethylene glycol tetra-acetic acid, 1 mM dithiothreitol (DTT), 1 mM Na_3VO_4, protease inhibitors, 1 mM phenylmethylsulfonylfluoride (PMSF), and ethylenediaminetetraacetic acid (EDTA)-free cocktail tablet] with periodic shaking on a vortex for 30 min. After centrifuging the cell lysates at 14,000 ×*g* for 15 min at 4 °C, protein supernatants were collected and stored at −70 °C until use. The corresponding protein concentration of each sample was determined using a BCA protein assay kit following the manufacturer's instruction (Pierce).

Proteins were separated by running on an 8%–12% SDS-PAGE gel and electro-transferred onto a nitrocellulose membrane, followed by

blocking in 5% non-fat dry milk/TBST (Tris-buffered saline buffer containing 0.1% Tween-20) for 1 h at room temperature. The membranes were incubated with primary antibodies against proinflammatory markers (IL-6, IL-8, IL-1β, and NFκB; 1: 1000, Novus Biologicals, Littleton, CO, USA), junction markers (ZO-1, occludin, and laudin-1; 1:1000, Cell Signaling Technology, Danvers, MA, USA), Notch-1 signaling markers (Notch-1, Hes-1, and jagged-1; 1:1000, Cell Signaling Technology), and β-actin (1:2000, Santa Cruz Biotechnology, CA, USA) diluted in TBST overnight at 4 °C. The blots were rinsed three times with TBST at 10 min intervals and incubated with horseradish peroxidase-conjugated secondary antibodies (rabbit, mouse, or goat; Dako, Glostrup, Denmark) in TBST for 1 h at room temperature. The band intensities were visualized using an enhanced chemiluminescence (ECL) detection kit following the manufacturer's instruction (Bio-Rad, CA, USA) and quantified using the Amersham ImageQuant 800 biomolecular imager (GE Healthcare Bio-Sciences, MA, USA), followed by quantitative analysis with normalization to the corresponding β-actin intensity.

2.13. qRT-PCR

Total RNA was extracted from cells and tissues using TRIzol (Invitrogen) following the manufacturer's instructions and quantified using a NanoDrop™ 2000 spectrophotometer (Thermo Fisher Scientific). Complementary DNA (cDNA) was produced using AccuPower® CycleScript RT Premix (Bioneer) according to the manufacturer's instructions using a T-100 Thermal Cycler (Bio-Rad) and subjected to PCR on a T100 Thermal Cycler (Bio-Rad) with a primer set and HiPi Plus 5 × PCR premix (Elpisbio), followed by agarose gel electrophoresis. qPCR was conducted using a cDNA, primer set, and SYBR Green PCR mix (Applied Biosystems) on a StepOne Plus Real Time PCR System (Applied Biosystems), followed by melting curve analysis. Each result was analyzed using the comparative Ct ($2^{-\Delta\Delta Ct}$) method and normalized to the expression of the corresponding glyceraldehyde 3-phosphate dehydrogenase (GAPDH). The sequences for the primes are listed in Table S1.

2.14. Statistical analysis

The data presentation style and the size of the biologically independent samples per group and/or the number of independent experiments are denoted in each figure and legend. Statistical differences between the experimental groups were analyzed using Excel and SigmaPlot V.8.0 (SPSS, Inc.). The significance of the differences between the two groups was determined using a two-tailed Student's t-test. Multiple comparisons among test groups were conducted using one-way analysis of variance (ANOVA), followed by post-hoc Bonferroni's analysis. Values of * $p < 0.05$, ** $p < 0.01$, and *** $p < 0.001$ were considered statistically significant.

3. Results

3.1. Determination of the Pe sequence as a flagellin mimic

Five Pe candidates with varying amino acid (a.a) sequences (3, 8, and 9 a.a) were identified from the flagellin D1 domain, and their binding affinities were quantitatively compared via a molecular docking study using Schrödinger software suite [17]. The binding status between TLR5 and each candidate was presented using a computational simulation with a multiple grid arrangement method, enabling the predictive visualization of the entire ligand-binding space (Fig. 1A). The computer simulation results suggested that the 8 and 9 a.a sequences were the best candidates because the binding efficiency parameters (docking score, glide score, glide model, and glide energy) had the most negative levels overall and thus presented the most superior binding efficiency among the candidates (Fig. 1B).

The binding efficiencies of the 8 and 9 a.a. sequences to the TLR5 were further compared using the 3 a.a. sequence as a control (Fig. 1C). When overexpression of the TLR5 was induced in human intestinal epithelial (Caco-2) cells by inflammation-inductive treatment, the 8 a.a. sequence exhibited the most incremental binding efficiency compared to Normal (i.e., before inflammatory activation) among the test candidates. The results were confirmed in detail by the largest amounts of the biotinylated 8 a.a. sequences with TLR5 post immunoprecipitation among the test groups, as seen in the western blot bands of the TLR5 (Fig. 1D). These results suggested that the 8 a.a. sequence was the best Pe to bind with the TLR5 and was used for the following experiments.

3.2. Pe-hydrogel synthesis and characterization

The hydrogel was synthesized through one-step ROP of mPEG and CL [9] (Fig. S2A). The molecular weight was controlled with 1–1.2 PDI to enable efficient sol-gel transition by varying the catalyst-to-monomer ratio, temperature, and reaction time (Fig. S2B). When the catalyst-to-monomer ratio increased, the molecular weight increased most effectively ($R^2 = 0.9752$) (Fig. S2C). Pe conjugation to the hydrogel was conducted at the site where the hydroxyl group of mPEG-PCL was aminated (Fig. 2A), followed by confirmation of the successful Pe conjugation with the chemical structure of the hydrogel by 1H NMR spectra (Fig. 2B). The hydrogel loaded and released Dex as a model drug in the modified transwell setting (Fig. S2D). As the mPEG-PCL concentration decreased from 10% to 6%, the amount of the Dex release increased up to 98.7% during 48 h in the HPLC analysis.

Nanomicelle formation was programmed to occur with the sol-gel transition after heating the amphiphilic mPEG-PCL polymers above the lower critical solution temperature (LCST, > 30 °C), indicating a drug cargo function by loading hydrophobic drugs (Fig. 2C). These properties indicated that the Pe-hydrogel could moisturize the intestinal epithelium using endoscopy or a syringe for IBD lesion-specific therapy, which relies on the Pe binding to TLR5 during inflammatory overexpression (Fig. 2D). During the temperature sweep, the hydrogels underwent efficient sol-gel transitions (Fig. S2E). When the hydrogel concentration was increased from 5% to 10%, its elastic modulus was improved with no significant change in the elasticity, indicating that around 5%–10% of the hydrogel concentration was in the target range for injection or spraying. In the gel state of the hydrogel, nanomicelle formation was visualized by SEM with an average diameter of ~100 nm, as analyzed by TEM and DLS (Fig. 2E). As a model drug, green fluorescence (Alexa Fluor™ 488 NHS Ester) could also be conjugated into hydrogel nanomicelles (Fig. 2F).

When Caco-2 cells were activated to overexpress TLR5, the 8 a.a.-hydrogel reduced the inflammatory action most effectively compared to no treatment among the test hydrogel groups, as evidenced by the suppression of TNF-α and NFκB expression at the gene and protein levels (Figs. S3A–B). The results were further supported by the Pe-hydrogel co-localization in Caco-2 cells as opposed to the hydrogel localization after the induction of TLR5 overexpression (Fig. 1E). These results suggest potential anti-inflammatory effects of Pe-hydrogel even without drug loading.

3.3. Therapeutic effects of Pe-hydrogel in a mouse IBD model

As an IBD model, colitis was induced in mice by feeding drinking water containing 3% DSS for the first 5 days until each mouse lost 10%–15% of its body weight (Fig. 3A and Fig. S4A). Mice were then provided with normal water from day 6, not fed for one day, and then a stool test was performed and were subjected to syringe injection of the hydrogel or Pe-hydrogel (8 wt/vol % in PBS) into the intestine on day 7, after which the body weight was measured daily for 11 days. When the weight was recovered to a normal range in the DSS w/Pe-hydrogel group, the mice were sacrificed on day 18 if they survived and then compared with the normal mouse group.

As the colon length decreases in response to the severity of the IBD,

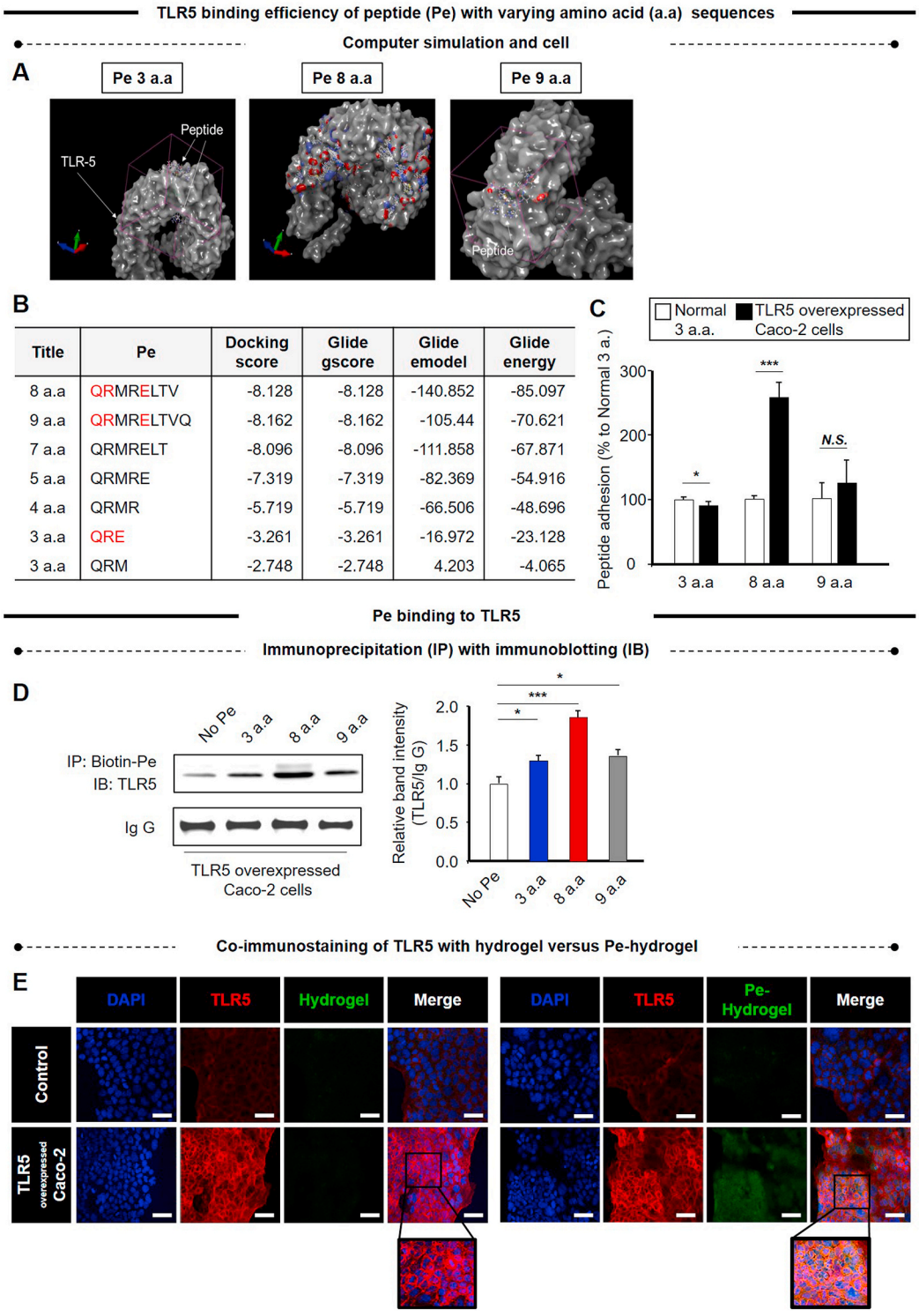

Title	Pe	Docking score	Glide gscore	Glide emodel	Glide energy
8 a.a	QRMRELTV	-8.128	-8.128	-140.852	-85.097
9 a.a	QRMRELTVQ	-8.162	-8.162	-105.44	-70.621
7 a.a	QRMRELT	-8.096	-8.096	-111.858	-67.871
5 a.a	QRMRE	-7.319	-7.319	-82.369	-54.916
4 a.a	QRMR	-5.719	-5.719	-66.506	-48.696
3 a.a	QRE	-3.261	-3.261	-16.972	-23.128
3 a.a	QRM	-2.748	-2.748	4.203	-4.065

Fig. 1. Determination of peptide (Pe) sequence to bind TLR5 efficiently as an effective flagellin mimic. (A) Binding status between TLR5 and Pe with varying amino acid (a.a) sequences (3, 8, and 9 a.a) as presented by a computational simulation using the multiple grid arrangement method. Red dots indicate a predicted peptide binding site, and blue dots indicate receptor grids for peptide docking. The multiple grid arrangement method enabled the predictive visualization of the entire ligand-binding space. **(B)** As a result of the computer simulation, the peptide candidates were selected by analyzing the binding efficiency parameters (Docking score, Glide gscore, Glide model, and Glide energy). As each parameter value becomes more negative, the binding efficiency increases. **(C)** The binding efficiency of selected candidates to TLR5 was determined by comparing Pe adhesion to human intestinal epithelial (Caco-2) cells before and post TLR5 overexpression by inflammation-inductive treatment. The results were confirmed by **(D)** immunoprecipitation of the biotinylated Pe candidates with TLR5, followed by western blotting of TRL5 for quantitative analysis, and **(E)** immunostaining of the co-localization between (Pe-) hydrogel (green) and TLR5 (red) in the Caco-2 cells (blue) after TLR5 over-expression. Scale bar = 50 μm. Data = mean ± standard deviation (SD) (n = 3). *$p < 0.05$, **$p < 0.01$, and ***$p < 0.001$ between lined groups. (For interpretation of the references to color in this figure legend, the reader is referred to the Web version of this article.)

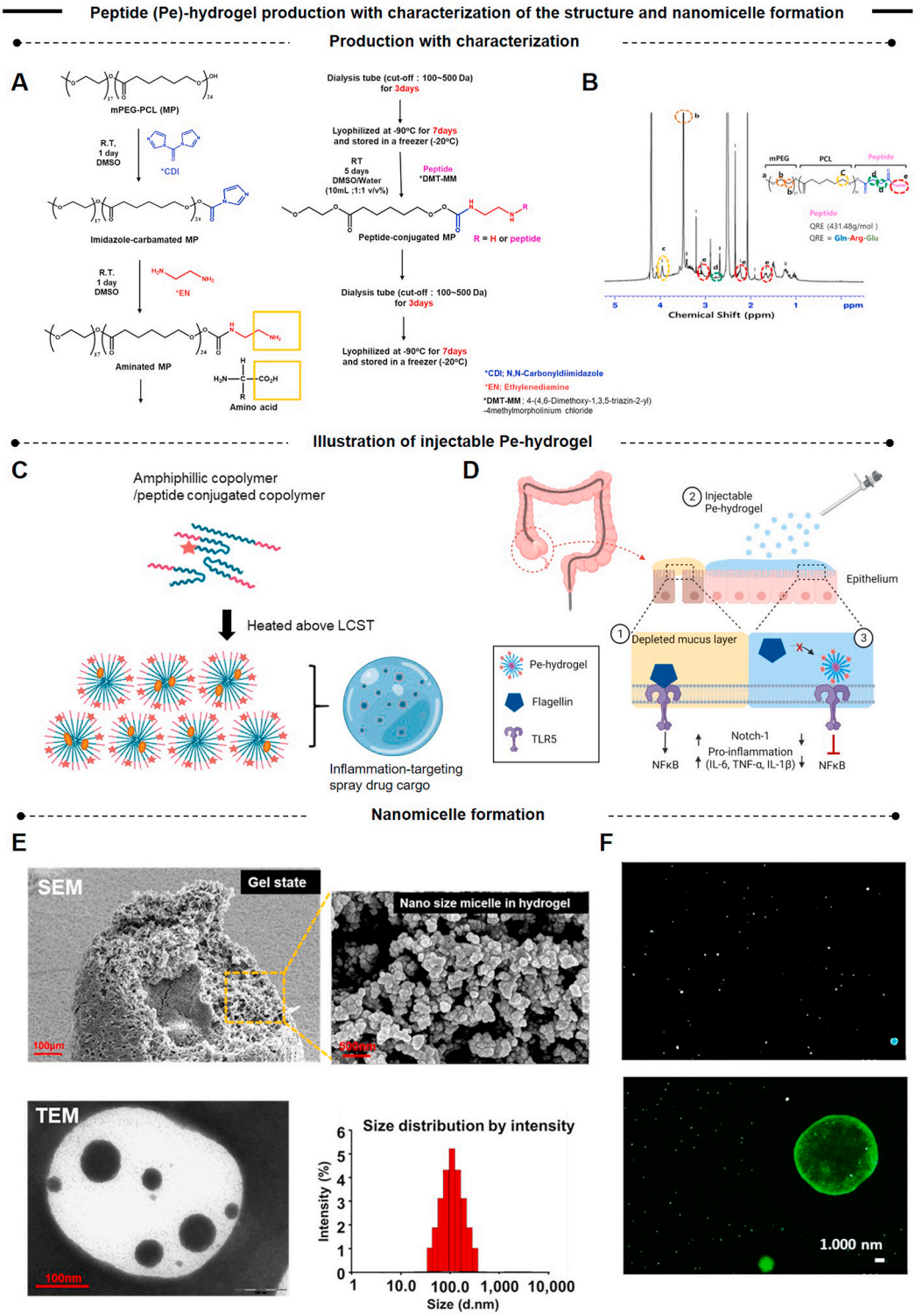

Fig. 2. Peptide (Pe)-hydrogel production with the characterization of the chemical structure and nanomicelle formation. (A) To produce Pe-hydrogel, first, the hydroxyl group on one side of mPEG-PCL was aminated using ED via the imidazole displacement of SN2 reaction with CDI. Then, peptides were conjugated to the aminated site via a condensation reaction using DMT-MM. **(B)** The successful production of Pe-hydrogel was confirmed by 1H NMR spectra using chloroform-d_6, in which the methyl and methylene groups of PEG appeared at 3.53 and 3.68 ppm, respectively. The peaks at 4.21–4.39, 3.73, 2.09–2.12, and 3.10–1.97 ppm were attributed to PCL with the peptide peak at 1.70 ppm for the –CH2- of arginine. **(C)** As illustrated, nanomicelles can be formed by heating amphiphilic PCL-mPEG polymers above the LCST (>30 °C), thereby serving as a drug cargo by loading hydrophobic drugs. **(D)** These properties enable spraying and injection of Pe-hydrogel to moisturize the intestinal epithelium by endoscopy and using a syringe for IBD lesion-specific therapy, as Pe binds to TLR5 during inflammatory over-expression. **(E)** At the gel state of hydrogel, nanomicelle formation was visualized by SEM and found to have a ~100 nm average diameter using TEM (left) and DLS (right). **(E)** As a model drug, green fluorescents (Alexa Fluor™ 488 NHS Ester) were loaded into nanomicelles via conjugation with the hydrogel. (For interpretation of the references to color in this figure legend, the reader is referred to the Web version of this article.)

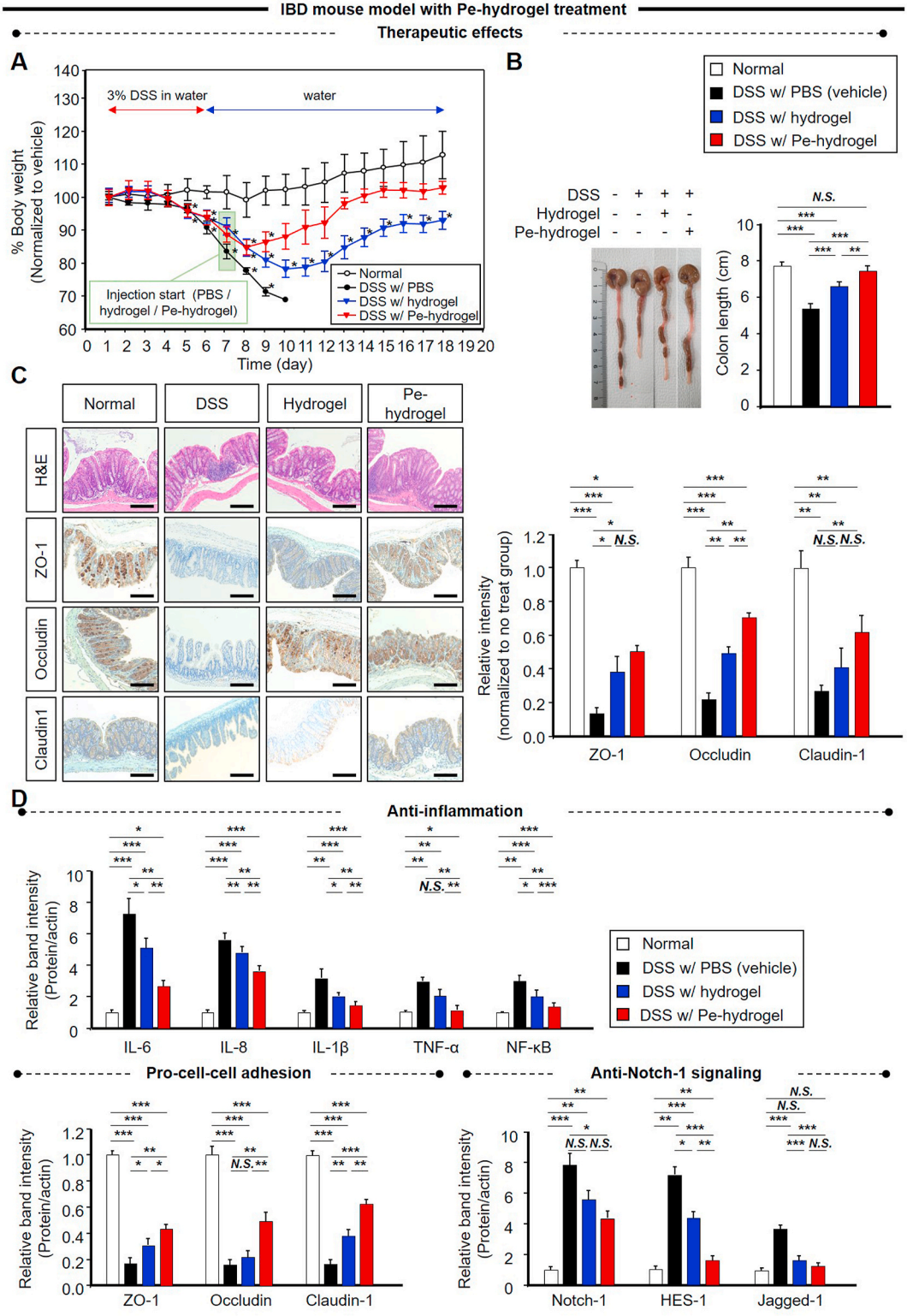

Fig. 3. Therapeutic effects of Pe-hydrogel in a mouse IBD model. (A) As an IBD model, drinking water containing 3% dextran sodium sulfate (DSS) was provided to induce colitis in mice until they lost 10–15% of their body weight. Then, normal water drinking was started at day 6, and feeding was stopped for one day, followed by a stool test. On day 7, hydrogel or Pe-hydrogel (8 wt/vol %) in PBS was administered for 11 days. After checking the weight recovery to a normal range in the DSS w/Pe-hydrogel group, mice were sacrificed at day 18 if they survived, as the vehicle control group (DSS w/PBS) died by day 10. The normal mouse group served as a control of IBD induction. **(B)** As anti-shortening of the colon indicates a therapeutic effect, colon lengths were compared quantitatively among the test groups. **(C)** In the colon tissues, the expression of tight junction markers (ZO-1, occludin, and claudin-1) was analyzed quantitatively by immunostaining to assess the recovery of barrier functions in the intestines post-inflammatory induction. Scale bar = 100 μm. **(D)** As IBD-specific therapeutic effects, protein expression of inflammation, cell-cell adhesion, and Notch-1 signaling markers was analyzed using western blotting. Data = mean ± standard error of mean (S.E.M) (Normal groups n = 8, DSS w/PBS groups n = 8, DSS w/hydrogel groups n = 13, DSS w/Pe-hydrogel groups n = 8). *$p < 0.05$, **$p < 0.01$, and ***$p < 0.001$ versus normal or between lined groups.

the therapeutic effects of Pe-hydrogel were evidenced by preserving the colon length to the normal level compared to that of the other test groups (Fig. 3B and Fig. S4B). Pe-hydrogel treatment also improved the barrier function of the intestine post-inflammatory induction, as evidenced by the increased expression of the tight junction protein markers (ZO-1, occludin, and claudin-1) in the colon tissues most closely to the normal levels compared to that of the other test groups (Fig. 3C). Moreover, Pe-hydrogel treatment exerted IBD-specific therapeutic effects by reducing inflammation, promoting cell-cell adhesion, and silencing Notch-1 signaling, as indicated by the most comparable expression of the protein markers to the normal group compared to that of the other test groups in the western blotting (Fig. 3D and **S4C).** This Pe-hydrogel effect also helped mice maintain a more intact barrier structure with less macrophage invasion, as seen in the images of the H&E histology and immunohistochemistry of the intestine (Fig. S4D and **S4E)**. These effects were driven by a sufficient therapeutic duration, as indicated by the inner-intestinal distribution of Pe-hydrogel with the Alexa-488 probe at day 18 post-injection by in vivo imaging system (IVIS) (Fig. S4F).

3.4. IBD patient cells, gut chip, and endoscopic injection

To validate the therapeutic potential of Pe-hydrogel for clinical translation, normal and IBD cells were isolated from the healthy and IBD lesions of patient-donated fresh colonic tissues, respectively. Pe-treatment significantly reduced inflammation, promoted cell-cell adhesion in the intestinal barrier function, and silenced Notch-1 signaling in IBD patient-derived cells upon 2D culture, as evidenced by the expression of protein markers compared to that of the w/o Pe-hydrogel group in western blot analysis. Normal patient-derived cells showed the healthiest indicators among the test groups (Fig. 4A and **S5A). (B)** The mechanistic roles of Notch-1 and TLR5 in inducing proinflammation and anti-cell-cell adhesion were validated through knockdown of the two signaling molecules using siRNAs in comparison with the scrambled siRNA-treated group (Fig. 4B and Fig. S5B). As a more realistic IBD model, a gut chip was used to culture the patient cells with and without Pe-hydrogel treatment (Fig. 4C and **S6A)**. Pe-hydrogel treatment for 96 h induced significant structural recovery of the IBD patient cells in the gut chips, as evidenced by the improved villi formation and ZO-1 expression compared to that of the w/o Pe-hydrogel group. The structural recovery appeared to accompany a reduction in proinflammatory cytokine release with increases in the villi height, resulting in improved TEER (Fig. 4D).

The same therapeutic effects of Pe-hydrogel on villi formation, cytokine release, villi height, and TEER value were confirmed in Caco-2 cells after the DSS treatment (Figs. S6B–C). Those therapeutic parameters recovered to the levels of the No DSS group upon Pe-hydrogel treatment for 48 h. As Pe-hydrogel was designed to be injected by endoscopy in the clinic, Pe-hydrogel was used to load a fluorescent dye (FITC green) and India ink (blue) and then sprayed onto the colon wall of the pig during colonoscopy (Fig. 4E and Movie S1). The injection efficiency was evidenced by the stable spreading of the ink over the wall. Then, Pe-hydrogel nanomicelles (FITC green) invaded the intestinal wall while preserving the barrier structure, as seen in the fluorescence and H&E imaging (Fig. 4F). The results indicate the clinical utility of Pe-hydrogel towards the development of an IBD lesion-specific all-in-one therapy.

Supplementary data related to this article can be found at https://doi.org/10.1016/j.bioactmat.2022.03.031.

3.5. Notch-1 therapeutic mechanism of Pe-hydrogel

As another cell model to validate the IBD mouse and patient cell results, Caco-2 cells were activated to overexpress TLR5 by TNF-α treatment (Fig. S7A). The treatment condition of TNF-α was determined to be 10 ng/mL for 24 h as the expression of both IL-6 and IL-8 proteins reached their highest levels in response to the incremental concentration and treatment time, compared to that of the normal group (w/o TNF-α). The therapeutic effects of Pe-hydrogel treatment were also confirmed by significantly reducing the expression of proinflammatory protein markers while promoting the consequent expression of cell-cell adhesion markers compared to those of the hydrogel treatment (Fig. 5A and **S7B)**. The inflammatory activation resulted in TLR5 overexpression, serving as a core docking site for the Pe-hydrogel in IBD lesions. As the TLR5-mediated inflammatory action results in the operation of the TNFα mechanism, a co-binding molecule may exist, such as Notch-1, also playing a regulatory role in the TNFα mechanism [14,23]. Hence, this mechanistic association was validated as Notch-1 expression increased in response to TLR5 overexpression (Figs. 5B and S7C) with a clear IP of the Pe-hydrogel and Notch-1 (Fig. 5C and **S7D)** compared to No treat.

Among the test groups, the Pe-hydrogel treatment reduced the protein expression of Notch-1 signaling mediators most closely to the levels of the normal group post-TNF-α treatment (Fig. 5D and **S7E)**. As Notch-1 expression was knocked down using siRNA, the effects of binding between Pe-hydrogel and Notch-1 to reduce the proinflammatory TNF-α actions disappeared compared to those of the scramble siRNA-treated group (Fig. 5E and **S7F)**. Hence, when Caco2 cells were co-treated with TNF-α and Pe-hydrogel, the increased production of proinflammatory markers and the decreased expression of cell-cell adhesion markers resulting from TNF-α treatment were maintained**.** Moreover, the co-operative role of TLR5 with Notch-1 in operating the anti-inflammatory effects of Pe-hydrogel treatment was also validated by the double knockdown of the two molecules (Fig. 5F and Fig. S7G). Notch-1 signaling is associated with TLR5 action through a downstream NF-κB mechanism, inducing inflammation (Fig. S7H). Hence, the therapeutic actions of Pe-hydrogel against IBD appeared to be driven by the binding of TLR5 with Pe, as a mimic of flagellin, suppressing NFκB-mediated inflammation, which exerted anti-Notch-1 effects together. The direct binding of Pe to Notch-1 and the suppression of downstream signaling by HES-1 potently supported this anti-inflammatory mechanism.

4. Discussion

The transitional gap from the bench to the clinic has been widely recognized in biotechnology. For the past decades, R&D sides have focused on developing more advanced technologies to overcome this gap. Despite continuous progress, it has been increasingly realized that repositioning existing therapeutics or devices could help solve the existing problems and accelerate the translational process within the R&D efforts. As a stellar example of this idea, the diagnostic function of endoscopy has been merged with a surgical option to remove polyps or tumors during on-site monitoring. This endoscopic polypectomy process requires injection of epinephrine solution underneath the intestinal wall tissue to minimize unnecessary bleeding [24], which can also be repositioned to inject therapeutics. Thus, diagnostic monitoring and pre-surgical therapeutic injection can be performed during endoscopic check-ups of potential IBD patients. Although lab tests (e.g., anemia/infection and stool) provide general IBD information [25], the endoscopic procedure represents an accurate diagnostic method to examine the entire intestine, including colon by colonoscopy, rectum, sigmoid by sigmoidoscopy, and duodenum by upper endoscopy. Hence, the theranostic function of endoscopy was suggested in this study as a foundation for new avenues for the IBD clinic.

The theranostic option for endoscopy can be advanced by further applying the concept of an all-in-one solution. This approach was suggested by combining punchline benefits from other potential IBD treatment ways including nanomedicines such as CeO2 [26] and Prussian blue [27], and hydrogels [28] to maximize the application-specific utility. A hydrogel can be sprayed using the solution-to-gel transition property to moisturize a large portion of the intestine, thereby covering the potential area related to IBD pathogenesis, representing a beneficial

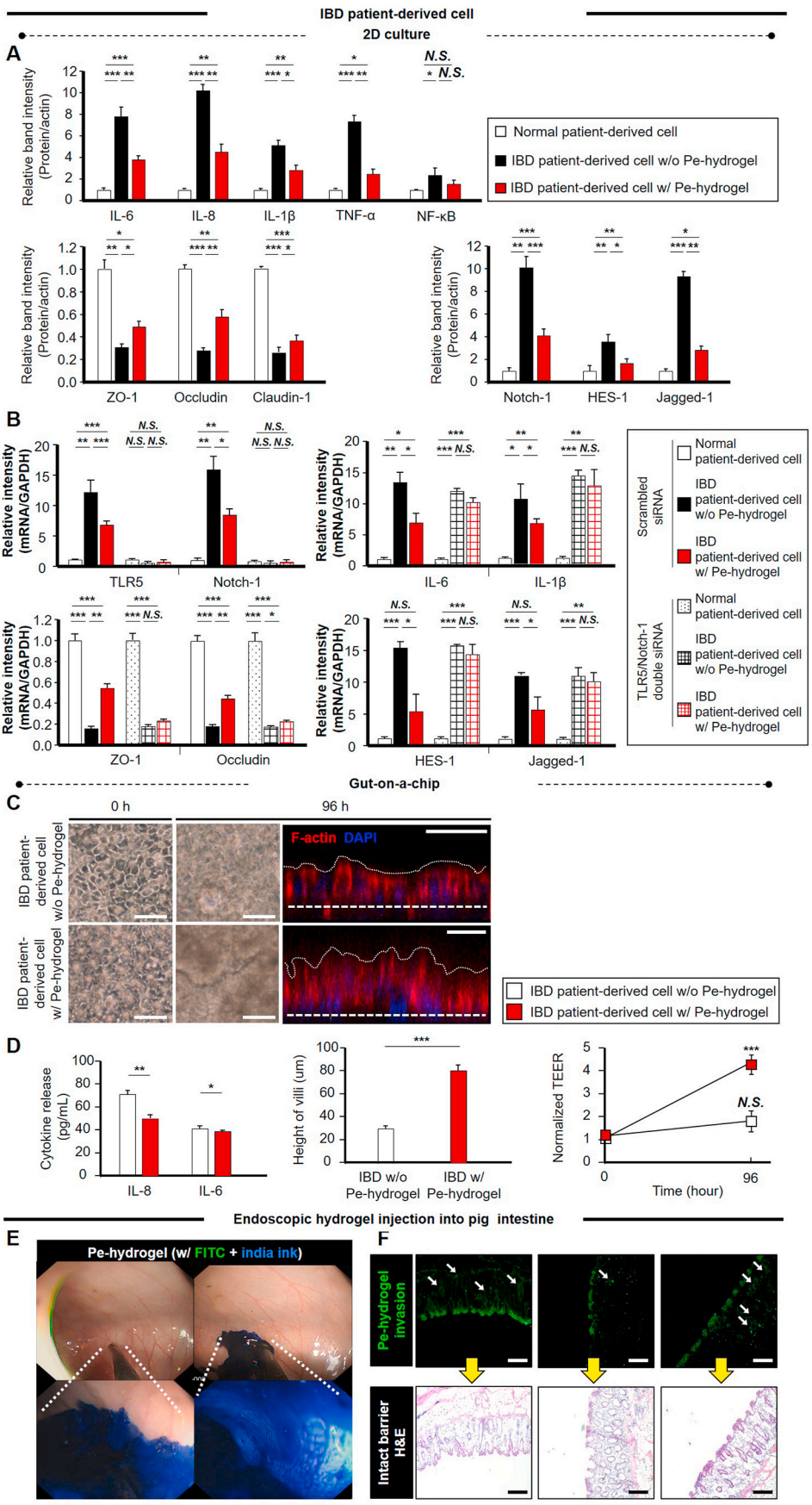

Fig. 4. Use of IBD patient cell, gut chip, and pigs to verify the therapy and injectability of Pe-hydrogel. (A) IBD and normal cells were isolated from IBD and healthy lesions of patient-donated fresh colonic tissues, respectively. Their responses to hydrogel treatment versus Pe-hydrogel were compared regarding protein expression of inflammation, cell-cell adhesion, and Notch-1 signaling markers using western blotting with quantitative analysis. **(B)** The mechanistic roles of Notch-1 and TLR5 in inducing proinflammation and anti-cell-cell adhesion were validated through knockdown of the two signaling molecules using siRNAs by qRT-PCR analysis in comparison with the scrambled siRNA-treated group. **(C)** A gut chip model was applied to culture the patient cells with and without Pe-hydrogel treatment as a more realistic IBD model. As an indication of structural recovery, villi formation was determined by phase-contrast (top view) and fluorescence (side view) imaging with immunostaining at 0 h and 96 h after Pe-hydrogel treatment. White dashed and dotted lines indicate porous basement membranes and the contours of villous microarchitectures, respectively. Scale bar = 50 μm. **(D)** Cytokine release, villi height, and barrier function were determined using ELISA (left), image analysis (middle), and the TEER system (right). Data = mean ± S.E.M (n = 3). *$p < 0.05$, **$p < 0.01$, and ***$p < 0.001$ between lined groups or versus the 0 h group. **(E)** To determine the clinical utility using pig intestines, a fluorescent dye (FITC green) and India ink (blue) were loaded into Pe-hydrogel and sprayed onto the colon wall of each pig using colonoscopy. The injection efficiency was evidenced by stable spreading of the ink over the wall. **(F)** Then, the subsequent invasion (white arrow) of Pe-hydrogel nanomicelles (FITC green) into the intestine wall as an indication of preserving the barrier structure (H&E) was demonstrated by imaging. Scale bar = 200 μm. (For interpretation of the references to color in this figure legend, the reader is referred to the Web version of this article.)

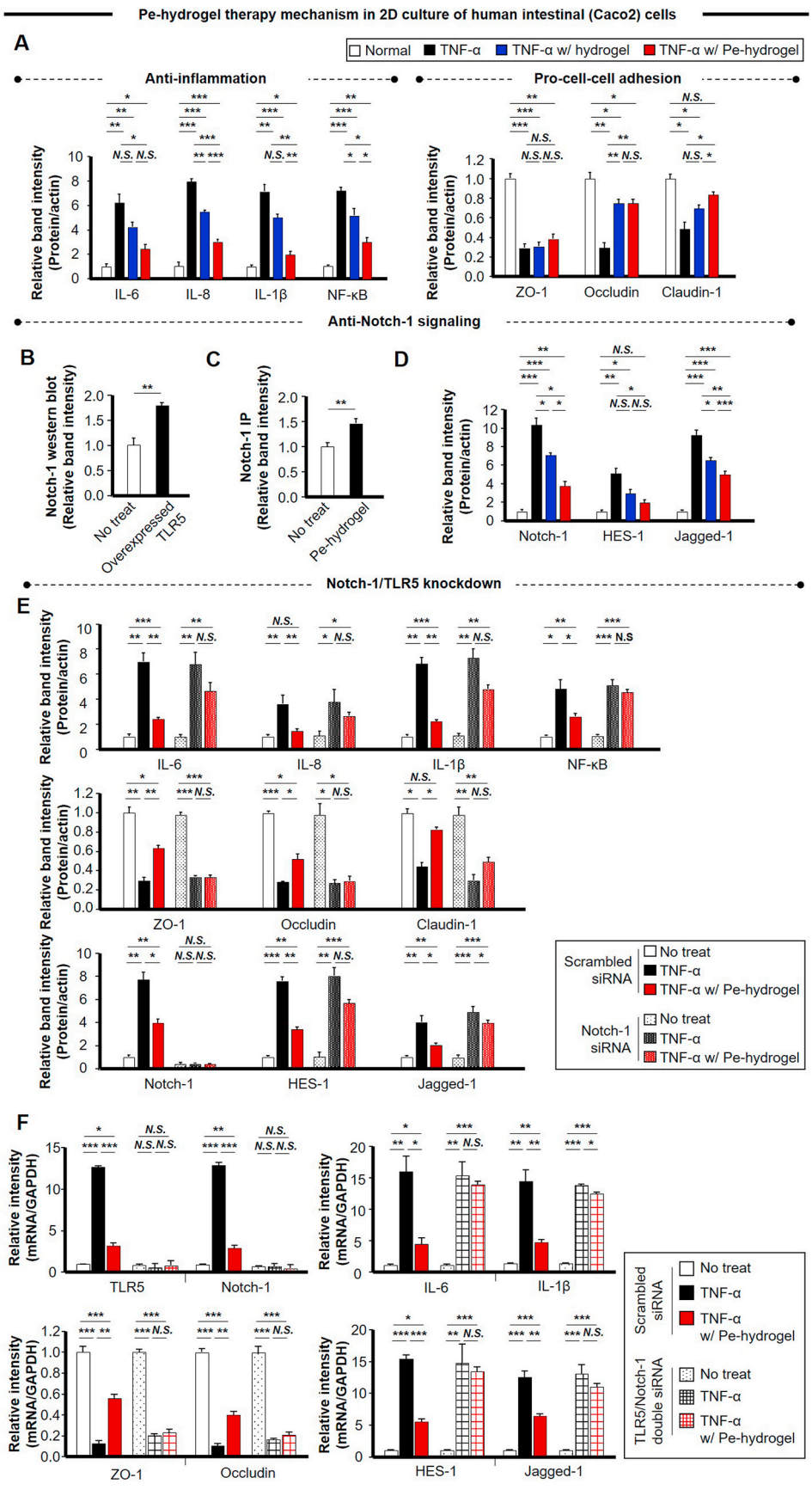

Fig. 5. Notch-1 as a key mediator of Pe-hydrogel therapeutic mechanism. Human intestinal epithelial cell line (Caco-2) was subjected to inflammatory activation by TNF-α treatment with consequent overexpression of TLR5 to validate the IBD mouse and patient cell results. The normal group was not exposed to TNF-α. Western blot analyses produced all readouts. Notch-1 signaling is associated with TLR5 action through a downstream NF-κB mechanism, inducing inflammation. **(A)** The effects of hydrogel versus Pe-hydrogel treatment on protein expression of inflammation and consequent cell-cell adhesion markers were compared. Then, the mechanistic association was determined by **(B)** an increase in Notch-1 expression in response to TLR5 overexpression and **(C)** immunoprecipitation to determine the binding between Pe-hydrogel and Notch-1. **(D)** Among the test groups, Pe-hydrogel treatment reduced the protein expression of Notch-1 signaling mediators most significantly post-inflammatory induction by TNF-α treatment. **(E)** As Notch-1 expression was knocked down using siRNA, the effects of binding between Pe-hydrogel and Notch-1 to reduce the proinflammatory TNF-α actions disappeared when compared to those of the scramble siRNA-treated group with **(F)** validation of the co-operative role of TLR5 with Notch-1 in mediating the anti-inflammatory effects of Pe-hydrogel treatment by double knockdown of the two molecules through qRT-PCR analyses. Data = mean ± S.E.M (n = 3). *p < 0.05, **p < 0.01, and ***p < 0.001 versus No treat or between lined groups.

utility of injectable hydrogel. Furthermore, the gel can adhere to IBD lesions specifically through Pe binding with TLR5 and Notch 1 and subsequently release nanomicelles to invade the lesions, thereby intensifying and prolonging the therapeutic effects based on the benefits of nanomedicine. Pe binding with the two molecules provides a touch-on start of potent anti-inflammatory signaling collaboratively. This step utilizes the concept of stimuli-responsive therapeutic activation [29] because overexpression of TLR5 is induced by inflammatory flagellin infection and serves as an initiation point of anti-inflammatory effects, which was potentiated further by the cross-activation of anti-inflammatory Notch 1 signaling. The whole set of ideas with the result validation suggests an unprecedented value to renovate the clinical treatment for IBD and the field of biomaterial-based therapy with collective merits of hydrogel and nanomedicine.

The clinical utility of Pe-hydrogel was demonstrated: i) using IBD patient cells in gut chips and ii) by intestinal injection and imaging during pig colonoscopies, as human and large animal models, respectively. Although the unique collaboration between clinicians (i.e., IBD pathology) and vegetarians (i.e., animal works) is significant and novel, human patients and pig IBD models could not be approached because the present research could not yet reach the stage of clinical investigation, and an IBD model of large animals could not be found in the literature search. In addition, the hydrogel itself without Pe conjugation appeared to exert some degree of therapeutic effects, suggesting a promising option to apply depending on the pathological stage of IBD progress. Hence, the physical support of hydrogel to enhance the intestinal barrier function should be investigated by varying the material properties (e.g., hydrogel concentration, modulus, protein repellency, and nanomicelle size) in a follow-up study.

In contrast, the activation of a single molecule in nature is associated with more than one downstream signaling and thereby possesses the potential to intensify therapeutic signaling and/or generate side effects. Pe binding suppressed Notch 1 signaling and downstream actions, and the results validated the anti-inflammatory effects. However, this signaling change may result in other unexpected effects such as anti-angiogenesis and anti-tumorigenesis, as was reported in a previous study [1], and should be investigated in greater detail in the future. In addition, the DSS was used to produce a mouse IBD model following previous studies [30]. Other reagents such as polyinosinic-polycytidylic acid and 2,4,6-trinitrobenzene sulfonic acid could be used to exert the same pathogenic effects and thereby produce rodent IBD models [31,32]. Hence, further studies are required to examine whether the therapeutic effects of Pe-hydrogel could be applied regardless of the model type. Moreover, the results indicated meaningful therapeutic effects of the hydrogel-only group (Fig. 3). Our previous study showed that the same hydrogel-only group adhered onto the epithelial surface of the gut in the DSS-treated mice [33]. Therefore, the barrier function could be physically improved by the hydrogel adhesion, resulting in subsequent recovery of cell-cell interaction with attenuation of inflammatory damages. Interestingly, the hydrogel-only group also induced anti-Notch-1 signaling, which requires further investigation in the future.

5. Conclusion

This study demonstrated the concept of all-in-one IBD theranostics by repositioning two bioactive materials in combination. First, the peptide sequence was programmed through *in silico* analyses to bind to TLR5 and thereby exert therapeutic anti-inflammatory effects by silencing the TLR5 signaling. Second, in collaboration with the peptide and hydrogel functions, the injectability of Pe-hydrogel was applied to spray on the inflamed regions of intestinal walls through the body temperature-responsive sol-gel transition process during endoscopy. The inflamed region-specific adhesion enabled IBD spots to detect and intensify therapeutic effects onto the spots. The Pe-hydrogel gelation upon adhesion helped the infected intestinal wall recover the barrier function physically. Moreover, the nanomicelle nature of hydrogel supported the invasion into the intestinal wall in co-operation with the peptide function, thereby prolonging the therapeutic effects by delivering the Pe-hydrogel further into the inside of the inflamed intestinal wall. The synergistic actions of peptide and hydrogel were validated in in vitro, in vivo, and human cell-chip experimental models of IBD versus the normal context, representing another aspect of translational research significance. As already mentioned, as a large animal model of IBD (e.g., pig) does not exist currently, validation of the Pe-hydrogel theranostic function and mechanism in this model remains to be conducted in the future.

Data and materials availability

All data are available in the main text or the Supplementary Materials.

Funding

The work was supported by the Bio & Technology Development Program of the National Research Foundation (NRF) funded by the Korean government (MSIT) [grant number 2019R1A2C2010802] to H.-J.S.; the Korea Medical Device Development Fund Grant funded by the Ministry of Science and ICT, the Ministry of Trade, Industry and Energy, the Ministry of Health & Welfare, the Ministry of Food and Drug Safety [grant number 1711138302, KMDF_PR_20200901_0152] to H.-J.S.; partly by the Starting Growth Technological R&D program of SMBA [grant number S2798389] to C.-S.K.; partially by the National Cancer Institute of the National Institutes of Health [grant number R21CA236690] to H.J.K.

CRediT authorship contribution statement

Hyo-Jin Yoon: Software, Data curation, Validation, Writing – original draft, Methodology. **Songhyun Lee:** Software, Data curation, Validation, Writing – original draft, Methodology. **Tae Young Kim:** Software, Data curation, Validation, Writing – original draft, Methodology. **Seung Eun Yu:** Investigation, Validation. **Hye-Seon Kim:** Investigation, Validation. **Young Shin Chung:** Investigation, Validation. **Seyong Chung:** Investigation. **Suji Park:** Resources. **Yong Cheol Shin:** Methodology. **Eun Kyung Wang:** Investigation. **Jihye Noh:** Investigation. **Hyun Jung Kim:** Validation. **Cheol Ryong Ku:** Validation. **Hong Koh:** Validation, Data curation. **Chang-Soo Kim:** Formal analysis. **Joon-Sang Park:** Visualization, Conceptualization, Writing – review & editing. **Young Min Shin:** Conceptualization, Writing – review & editing. **Hak-Joon Sung:** Project administration, Supervision, Conceptualization, Writing – review & editing.

Declaration of competing interest

The authors declare that they have no known competing financial interests or personal relationships that could have appeared to influence the work reported in this paper.

Appendix A. Supplementary data

Supplementary data to this article can be found online at https://doi.org/10.1016/j.bioactmat.2022.03.031.

References

[1] H.S. Kim, Y.M. Shin, S. Chung, D. Kim, D.B. Park, S. Baek, J. Park, S.Y. Kim, D. H. Kim, S.W. Yi, Cell-membrane-derived nanoparticles with notch-1 suppressor delivery promote hypoxic cell–cell packing and inhibit angiogenesis acting as a two-edged sword, Adv. Mater. (2021) 2101558.

[2] S. Nagl, A. Ebigbo, S.K. Goelder, C. Roemmele, L. Neuhaus, T. Weber, G. Braun, A. Probst, E. Schnoy, A.J. Kafel, A. Muzalyova, H. Messmann, Underwater vs

Conventional Endoscopic Mucosal Resection of Large Sessile or Flat Colorectal Polyps: A Prospective Randomized Controlled Trial, 2021. Gastroenterology.
[3] L.R. Nih, S. Gojgini, S.T. Carmichael, T. Segura, Dual-function injectable Angiogenic biomaterial for the repair of brain tissue following stroke, Nat. Mater. 17 (2018) 642–651.
[4] L. Yu, W. Xu, W. Shen, L. Cao, Y. Liu, Z. Li, J. Ding, Poly(Lactic acid-Co-glycolic acid)-poly(ethylene glycol)-poly(lactic acid-Co-glycolic acid) thermogel as a novel submucosal cushion for endoscopic submucosal dissection, Acta Biomater. 10 (2014) 1251–1258.
[5] J.M. Pantshwa, P.P.D. Kondiah, Y.E. Choonara, T. Marimuthu, V. Pillay, Nanodrug delivery systems for the treatment of ovarian cancer, Cancers 12 (2020).
[6] S. Zhang, J. Ermann, M.D. Succi, A. Zhou, M.J. Hamilton, B. Cao, J.R. Korzenik, J. N. Glickman, P.K. Vemula, L.H. Glimcher, An inflammation-targeting hydrogel for local drug delivery in inflammatory bowel disease, Sci. Transl. Med. 7 (2015), 300ra128-300ra128.
[7] T.T. Jubeh, Y. Barenholz, A. Rubinstein, Differential adhesion of normal and inflamed rat colonic mucosa by charged liposomes, Pharm. Res. (N. Y.) 21 (2004) 447–453.
[8] T.-H. Kim, M.S. Kang, N. Mandakhbayar, A. El-Fiqi, H.-W. Kim, Anti-inflammatory actions of folate-functionalized bioactive ion-releasing nanoparticles imply drug-free nanotherapy of inflamed tissues, Biomaterials 207 (2019) 23–38.
[9] A.L. Zachman, X. Wang, J.M. Tucker-Schwartz, S.T. Fitzpatrick, S.H. Lee, S. A. Guelcher, M.C. Skala, H.J. Sung, Uncoupling angiogenesis and inflammation in peripheral artery disease with therapeutic peptide-loaded microgels, Biomaterials 35 (2014) 9635–9648.
[10] N. Jommanee, C. Chanthad, K. Manokruang, Preparation of injectable hydrogels from temperature and ph responsive grafted chitosan with tuned gelation temperature suitable for tumor acidic environment, Carbohydr. Polym. 198 (2018) 486–494.
[11] J.S. Kwon, S.W. Kim, D.Y. Kwon, S.H. Park, A.R. Son, J.H. Kim, M.S. Kim, In vivo osteogenic differentiation of human turbinate mesenchymal stem cells in an injectable in situ-forming hydrogel, Biomaterials 35 (2014) 5337–5346.
[12] L. Rhayat, M. Maresca, C. Nicoletti, J. Perrier, K.S. Brinch, S. Christian, E. Devillard, E. Eckhardt, Effect of Bacillus subtilis strains on intestinal barrier function and inflammatory response, Front. Immunol. 10 (2019) 564.
[13] S.I. Yoon, O. Kurnasov, V. Natarajan, M. Hong, A.V. Gudkov, A.L. Osterman, I. A. Wilson, Structural basis of tlr5-flagellin recognition and signaling, Science 335 (2012) 859–864.
[14] M. Aziz, S. Ishihara, M.U. Ansary, H. Sonoyama, Y. Tada, A. Oka, R. Kusunoki, Y. Tamagawa, N. Fukuba, Y. Mishima, T. Mishiro, N. Oshima, I. Moriyama, N. Ishimura, S. Sato, T. Yuki, K. Kawashima, Y. Kinoshita, Crosstalk between Tlr5 and Notch1 signaling in epithelial cells during intestinal inflammation, Int. J. Mol. Med. 32 (2013) 1051–1062.
[15] D.C. Baumgart, W.J. Sandborn, Inflammatory bowel disease: clinical aspects and established and evolving therapies, Lancet 369 (2007) 1641–1657.
[16] W.S. Song, Y.J. Jeon, B. Namgung, M. Hong, S.I. Yoon, A conserved Tlr5 binding and activation hot spot on flagellin, Sci. Rep. 7 (2017) 40878.
[17] R.A. Friesner, J.L. Banks, R.B. Murphy, T.A. Halgren, J.J. Klicic, D.T. Mainz, M. P. Repasky, E.H. Knoll, M. Shelley, J.K. Perry, D.E. Shaw, P. Francis, P.S. Shenkin, Glide: a new approach for rapid, accurate docking and scoring. 1. Method and assessment of docking accuracy, J. Med. Chem. 47 (2004) 1739–1749.
[18] H.M. Berman, J. Westbrook, Z. Feng, G. Gilliland, T.N. Bhat, H. Weissig, I. N. Shindyalov, P.E. Bourne, The protein Data Bank, Nucleic Acids Res. 28 (2000) 235–242.
[19] I. Tubert-Brohman, W. Sherman, M. Repasky, T. Beuming, Improved docking of polypeptides with glide, J. Chem. Inf. Model. 53 (2013) 1689–1699.
[20] Y. Chen, X. Chen, Y. Chen, H. Wei, S. Lin, H. Tian, T. Lin, J. Zhao, X. Gu, Preparation, characterisation, and controlled release of sex pheromone-loaded mpeg-pcl diblock copolymer micelles for spodoptera litura (Lepidoptera: noctuidae), PLoS One 13 (2018), e0203062.
[21] X. Wang, H. Hu, W. Wang, K.I. Lee, C. Gao, L. He, Y. Wang, C. Lai, B. Fei, J.H. Xin, Antibacterial modification of an injectable, biodegradable, non-cytotoxic block copolymer-based physical gel with body temperature-stimulated sol-gel transition and controlled drug release, Colloids Surf. B Biointerfaces 143 (2016) 342–351.
[22] H.J. Kim, D. Huh, G. Hamilton, D.E. Ingber, Human gut-on-a-chip inhabited by microbial flora that experiences intestinal peristalsis-like motions and flow, Lab Chip 12 (2012) 2165–2174.
[23] L. Werner, U. Berndt, D. Paclik, S. Danese, A. Schirbel, A. Sturm, Tnfα inhibitors restrict T cell activation and cycling via notch-1 signalling in inflammatory bowel disease, Gut 61 (2012) 1016–1027.
[24] T. Tullavardhana, P. Akranurakkul, W. Ungkitphaiboon, D. Songtish, Efficacy of submucosal epinephrine injection for the prevention of postpolypectomy bleeding: a meta-analysis of randomized controlled studies, Ann. med. surg. 19 (2017) 65–73.
[25] S. Vermeire, G. Van Assche, P. Rutgeerts, Laboratory markers in ibd: useful, magic, or unnecessary toys? Gut 55 (2006) 426–431.
[26] S. Zhao, Y. Li, Q. Liu, S. Li, Y. Cheng, C. Cheng, Z. Sun, Y. Du, C.J. Butch, H. Wei, An Orally Administered Ceo2@Montmorillonite Nanozyme Targets Inflammation for Inflammatory Bowel Disease Therapy 30, 2020, p. 2004692.
[27] J. Zhao, W. Gao, X. Cai, J. Xu, D. Zou, Z. Li, B. Hu, Y. Zheng, Nanozyme-mediated catalytic nanotherapy for inflammatory bowel disease, Theranostics 9 (2019) 2843–2855.
[28] H. Laroui, G. Dalmasso, H.T. Nguyen, Y. Yan, S.V. Sitaraman, D. Merlin, Drug-loaded nanoparticles targeted to the colon with polysaccharide hydrogel reduce colitis in a mouse model, Gastroenterology 138 (2010) 843–853, e841-842.
[29] H. Jin, C. Wan, Z. Zou, G. Zhao, L. Zhang, Y. Geng, T. Chen, A. Huang, F. Jiang, J.-P. Feng, Tumor ablation and therapeutic immunity induction by an injectable peptide hydrogel, ACS Nano 12 (2018) 3295–3310.
[30] L. Gao, Q. Yu, H. Zhang, Z. Wang, T. Zhang, J. Xiang, S. Yu, S. Zhang, H. Wu, Y. Xu, Z. Wang, L. Shen, G. Shu, Y.G. Chen, H. Liu, L. Shen, B. Li, A resident stromal cell population actively restrains innate immune response in the propagation phase of colitis pathogenesis in mice, Sci. Transl. Med. 13 (2021).
[31] R. Zhou, H. Wei, R. Sun, Z. Tian, Recognition of double-stranded rna by Tlr3 induces severe small intestinal injury in mice, J. Immunol. 178 (2007) 4548–4556.
[32] K. Scheibe, C. Kersten, A. Schmied, M. Vieth, T. Primbs, B. Carlé, F. Knieling, J. Claussen, A.C. Klimowicz, J. Zheng, Inhibiting interleukin 36 receptor signaling reduces fibrosis in mice with chronic intestinal inflammation, Gastroenterology 156 (2019) 1082–1097, e1011.
[33] I.G. Kwon, C.W. Kang, J.P. Park, J.H. Oh, E.K. Wang, T.Y. Kim, J.S. Sung, N. Park, Y.J. Lee, H.J. Sung, E.J. Lee, W.J. Hyung, S.J. Shin, S.H. Noh, M. Yun, W.J. Kang, A. Cho, C.R. Ku, Serum glucose excretion after roux-en-Y gastric bypass: a potential target for diabetes treatment, Gut 70 (2021) 1847–1856.